Geobiology

Geobiology (2010), **8**, 234–243 DOI: 10.1111/j.1472-4669.2010.00239.x

Subsurface characterization of methane production and oxidation from a New Hampshire wetland

J. K. SHOEMAKER[1] AND D. P. SCHRAG[2]

[1]*Harvard University Department of Organismic and Evolutionary Biology, Cambridge, MA, USA*
[2]*Harvard University Department of Earth and Planetary Sciences, Cambridge, MA, USA*

ABSTRACT

We measured the carbon isotopic composition of pore water carbon dioxide from Sallie's Fen, a New Hampshire poor fen. The isotope profiles are used in combination with a one-dimensional diffusion–reaction model to calculate rates of methane production, oxidation and transport over an annual cycle. We show how the rates vary with depth over a seasonal cycle, with methane produced deeper during the winter months and at progressively shallower depths into the summer season. The rates of methane production, constrained by the measured $\delta^{13}C_{dic}$ profiles, cannot explain high methane emission during the summer. We suggest that much of the methane produced during this time comes either from the unsaturated peat, or from the top 1–3 cm of saturated peat where episodic exchange with the atmosphere makes it invisible to our method.

Received 12 August 2009; accepted 28 February 2010

Corresponding author: J. K. Shoemaker. Tel.: (617) 495-2664; fax: (617) 496-4387; e-mail: jshoemak@fas.harvard.edu

INTRODUCTION

Freshwater wetlands are the largest non-anthropogenic source of methane to the atmosphere (Hein *et al.*, 1997; Denman *et al.*, 2007), and yet large uncertainties remain on both the magnitude of current emissions and the potential impact of climate change on these emissions (Wuebbles & Hayhoe, 2002). There are three important processes involved in methane emissions from wetlands (Conrad, 1989; Smith *et al.*, 2003) that remain difficult to separate and quantify: methane production, methane oxidation and transport mechanisms. A mechanistic understanding of these processes would greatly improve our ability to predict the fate of large soil carbon reservoirs in response to changing climate forcings.

Methane is produced under anoxic conditions by communities of methane-producing archaea (methanogens) and results in the production of equal quantities of CO_2 and CH_4. Methane is oxidized by bacteria (methanotrophs) in the oxic zone of the pore water, a process that consumes $2O_2$ for each CO_2 molecule evolved. Three modes of gas transport are also active in this system: diffusion, plant-mediated transport and ebullition (Holzapfel-Pschorn *et al.*, 1986; Whiting & Chanton, 1992; Bubier, 1995; Shannon *et al.*, 1996; Thomas *et al.*, 1996; Smith *et al.*, 2003).

Methanogens select against the heavier isotope of carbon (carbon-13) through a kinetic isotope fractionation; this results in produced methane that is depleted in ^{13}C by 20–60‰ relative to the source organic carbon and CO_2 that is enriched by the same amount. The absolute magnitude depends on the pathway through which methane is produced; either by splitting acetate ($CH_3COOH \rightarrow CO_2 + CH_4|\varepsilon = 25–35‰$), or by CO_2-reduction ($CO_2 + 4H_2 \rightarrow CH_4 + 2H_2O|\varepsilon \geq 55‰$) (Ferry, 1992; Gelwicks *et al.*, 1994; Whiticar, 1999). Epsilon is defined as $\varepsilon = 1000(\alpha_{process} - 1)$, and approximated as $\varepsilon \approx (\delta^{13}C_{substrate} - \delta^{13}C_{prod})$, as described in Whiticar (1999). For CO_2-reduction, it is easier to think about the reaction in two steps as follows (i) $2CH_2O + 2H_2O + e^-$ acceptor $\rightarrow 2CO_2 + 4H_2$ and (ii) $CO_2 + 4H_2 \rightarrow CH_4 + 2H_2O$. The sum of these two reactions is the same as methanogenesis from acetate, although the fractionation associated with the reaction is different. Methane can also be produced by other mechanisms, such as methylotrophy, but the contribution to methanogenesis is believed to be less important (Whiticar, 1999). Methane oxidation converts some of the produced CH_4 into CO_2 with an isotopic signature that is approximately 10‰ depleted relative to the source CH_4, although values as high as 27‰ have been observed (Teh *et al.*, 2006). Oxidative organic carbon respiration (and heterotrophic metabolism in general) is believed to yield

CO_2 of nearly the same isotopic composition as the source organic matter (Balesdent *et al.*, 1987; Penning & Conrad, 2006).

Much of the previous work on understanding production and oxidation rates have used laboratory incubations to determine potential rates under either reproduced *in situ* or idealized conditions (Phelps & Zeikus, 1984; Frolking & Crill, 1994; Bergman *et al.*, 1998; Duval & Goodwin, 2000; Blodau & Moore, 2003). Alternately, static flux chambers and eddy flux covariance techniques have been employed to look at surface fluxes followed by a correlation analysis with environmental variables to connect emissions with belowground processes (Goodwin & Zeikus, 1987; Conrad, 2002; Kang & Freeman, 2002; Blodau & Moore, 2003). Although much important information has been gathered this way, such surface flux calculations integrate the *in situ* processes making them difficult to separate and quantify, whereas laboratory incubations can introduce artefacts that alter the microbial communities from their natural state.

Several modelling studies have attempted to bridge this gap. In a model by Walter *et al.* (1996), methane production and oxidation rate functions are forced by water table and temperature in order to fit observed methane emission data from several sites (Walter & Heimann, 2000; Walter *et al.* 1996), but the rates of methanogenesis are not constrained by observations. Beer & Blodau (2007) employed a steady-state model (developed by Berg *et al.* (1998)) that relies on CH_4 concentration profiles to calculate rates of methane production under the peat surface. In this study, we use an inverse modelling strategy – a 1D diffusion–reaction model with no steady-state assumption– to calculate rates of methane production, oxidation and transport from a New Hampshire poor fen. The rates of (net) methanogenesis and (net) methanotrophy are constrained at each depth by the isotopic composition of the dissolved inorganic carbon (primarily $CO_{2(aq)}$ due to the acidity) that we measure throughout the year, which provides a time-averaged record of water-column processes. CO_2 is relatively undersaturated in the pore water compared with CH_4 and less subject to non-diffusive transport. The main use for the CH_4 concentration profiles is to help constrain the activity of the alternate transport pathways whereas the CO_2 concentrations help to discern between oxygenic respiration and methanotrophy. This method allows us to separate and quantify the rates of processes occurring *in situ* beneath the fen surface.

METHODS

The study site, Sallie's Fen, is located in Barrington, NH, USA (43°12.5′N, 71°03.5′W). Sallie's Fen is an NSF LTREB (Long Term Research in Environmental Biology) (Frolking & Crill, 1994; Treat *et al.*, 2007). Sallie's Fen is a 1.7 ha, mineral poor, bryophyte-dominated fen that receives most of its water from rainfall and runoff (Frolking & Crill, 1994; Melloh & Crill, 1996; Treat *et al.*, 2007). Although we do not measure the pH of each individual sample, pH measurements made on selected profiles with litmus paper have consistently shown a surface pH of approximately 4, increasing to 5 at about 60 cm below the water table. The water table varied seasonally at Sallie's Fen during 2006 by almost 40 cm. During the winter (January–May) the water table was about 20 cm below the peat surface, decreasing to 30 cm in June and remaining approximately 40 cm below the peat surface through October (it was an anomalously dry year). The water table then increased until it reached near the peat surface by December 2006. The sampling site has complete sphagnum cover with both *carex* and leatherleaf present. The *carex* and ericaceous shrubs together account for approximately 25% of the total vegetation cover in the nearest metre.

We collected pore water at Sallie's Fen monthly throughout 2006 at three to five different sites, each closely associated with a previously installed static flux chamber location. Results from only one site, Station 4, were the first to be analysed and are discussed exclusively in this study. We sampled the pore water using a stainless steel tube inserted into the peat through which pore water was pulled directly into 12 mL evacuated containers (Vacutainers®; Becton, Dickinson and Co. – the actual volume of these containers was found to be 13.2 mL including the space under the septum). Samples were drawn every 2.5–25 cm and every 5 cm thereafter. Sampling continued until the evacuated container failed to move pore water up the sampling tube (this depth varied between 50 cm and 1 m below the water table). The vials were allowed to fill approximately halfway (by eye) leaving 5–7 mL of headspace volume. Two replicate samples were taken at each depth. All depths in this study are reported relative to the depth at which the peat is fully saturated (water table). We do not know for certain whether or not our depth zones overlap, although the high hydraulic conductivity of peat discourages vertical flow with less resistance to lateral movement. At each depth, only 15 mL of water is removed, but it is possible that some overlapping of depths creates curves that are artificially smoother than those present *in situ*. All samples were stored on ice in a dark cooler until return to the laboratory where they were preserved with $HgCl_2$.

Concentrations of CO_2 and CH_4 were measured by injecting 500 μL of headspace gas from each sample into an HP 6890N gas chromatograph. The gas chromatograph was equipped with a 10′ unibead column linked through a 6-port valve to a 10′ molecular sieve 5A column. The columns either run in sequence into a thermal conductivity detector or the valve can be switched, skipping the second (molecular sieve) column. This system enables quantification of both CO_2 and CH_4 on a single sample injection. The lower detection limits for CO_2 and CH_4 respectively were estimated to be 0.2 and 0.1 mM. The GC output (calibrated to moles of CO_2 and CH_4) was converted to millimolar units in the following way: first, we assumed that all the CH_4 outgasses into the

headspace, and that the aqueous CO_2 partitions into the headspace and the water in accordance with its Henry's law constant (addition of 100% H_2PO_4 was found to have no effect on the CO_2 concentrations measured). Second, the volume of pore water in each sample was determined by weighing the vial, and the headspace volume calculated as the remainder volume plus the 500-μL injection volume. Using these steps, we can calculate the concentration of gases in both the headspace and the water volume and back-calculate the concentrations of CH_4 and CO_2 in the sampled pore waters. If we include the differences in the concentrations between vials collected sequentially at the same depth, we calculate uncertainties of 0.4 mM for CO_2 and 1.3 mM for CH_4. Measurement errors alone, calculated from external standards, were <0.2 mM for both CO_2 and CH_4. We believe that the true 1 SD uncertainty lies between these bounds. The isotopic composition of the pore water CO_2 was measured on a Thermo-Finnigan Delta Plus XL IRMS with combined measurement and sampling errors, based on internal and external standards and the reproducibility of replicate samples, of ±0.5‰.

Model description

We used a 1D diffusion reaction model to reproduce the concentration and isotope data collected from Sallie's Fen. Five compounds were tracked through the system: O_2, $^{12}CO_2$, $^{13}CO_2$, $^{12}CH_4$ and $^{13}CH_4$ through a column of 100 vertical boxes each representing 1 cm of soil depth. This modelling approach is similar to the one used in Sivan *et al.* (2007) on marine sediment core data and originates from a field of previous work (Berner, 1980; Schrag & DePaulo, 1993). Porosity is assumed to be constant with depth. Respiration, methane oxidation and methane production rates are manually input for each depth. Resolving the isotopic contribution from methane oxidation versus oxygenic respiration (both of which add depleted carbon) relies on the CO_2 concentration profiles as constraints, which results in larger uncertainties on the rates of methane oxidation than on the rates of methane production. Resolving the contribution from non-diffusive transport pathways relies on the CH_4 concentration profiles. Overall, we estimate an error on the calculated rate values from the model of approximately a factor of 3. Error in the model results is difficult to calculate precisely because it depends on uncertainties in different parameters and subjective weighting of the fits to the concentration and isotope data. Based on sensitivity tests to different parameter choices, such as the alpha value, we estimate the error to be <60% for seasonal trends and relative changes within profiles. Further detail on these sensitivity tests and the error estimates are available in Appendix S1.

Equations

The following coupled differential equations were solved using a centred finite difference approach. Time steps forward in half-an-hour intervals and the model runs for a year. Initial conditions are taken from data profiles collected from the month previous to the model start time (in this case, December 2005). Additional support for the model assumption that methane production results in a 1:1 ratio of CO_2:CH_4 is presented through sensitivity analysis in Appendix S1.

$$\frac{\partial^{12}CO_2}{\partial t} = D_{CO_2}\frac{\partial^{12}CO_2}{\partial z} + CH_4prod_{z,t} + CH_4ox_{z,t} + resp_{z,t}$$

$$\frac{\partial^{13}CO_2}{\partial t} = D_{CO_2}\frac{\partial^{13}CO_2}{\partial z} + (a_{prod-dic} \times CH_4prod_{z,t}) + (a_{ox-dic} \times CH_4ox_{z,t}) + (r_{org} \times resp_{z,t})$$

$$\frac{\partial CH_4}{\partial t} = D_{CH_4}\frac{\partial CH_4}{\partial z} + CH_4prod_{z,t} - CH_4ox_{z,t}$$

$$\frac{\partial^{13}CH_4}{\partial t} = D_{CH_4}\frac{\partial^{13}CH_4}{\partial z} + (a_{prod-ch4} \times CH_4prod_{z,t}) - (a_{ox-ch4} \times CH_4ox_{z,t})$$

$$\frac{\partial O_2}{\partial t} = D_{O_2}\frac{\partial O_2}{\partial z} - 2 \times CH_4ox_{z,t} - resp_{z,t}$$

$$r_{\aleph} = \frac{^{13}C_{\aleph}}{^{12}C_{\aleph}}$$

$$a_{prod-dic} = 0.75 \times \frac{r_{org}}{\alpha_{acetate\rightarrow dic}} + 0.25 \times \frac{r_{dic}}{\alpha_{co2red\rightarrow dic}}$$

$$a_{prod-ch4} = 0.75 \times \frac{r_{org}}{\alpha_{acetate\rightarrow ch4}} + 0.25 \times \frac{r_{dic}}{\alpha_{co2red\rightarrow ch4}}$$

$$a_{prod-dic} = \frac{r_{ch4}}{\alpha_{ox\rightarrow dic}}$$

$$a_{prod-ch4} = \frac{r_{ch4}}{\alpha_{ox\rightarrow ch4}}$$

Parameters

CH_4prod, CH_4ox and resp were each 100×10 vectors with assigned values for each depth associated with each month. They are not parameterized functions. There are only 10 distinct vectors due to lack of profile data from January and March; January was given the same vector as February and March was the given the same vector as April to account for the time integration of the $\delta^{13}C_{CO2}$ profiles. The values within each vector were manipulated manually, beginning with a 'best guess' profile, until the resulting model output reproduced the pattern of data collected, specifically the $\delta^{13}C_{CO2}$ profiles. If the model run failed to reproduce the data, the methane oxidation, production and respiration rates were adjusted, taking into consideration the isotope and concentration profiles, and the model was rerun. Values for all included parameters are given in Table 1. The respiration term was chosen to be non-zero

Table 1 Model parameter values

Variable	Value	Explanation or reference
D_{CO2}	2×10^{-5} cm^2 s^{-1}	Lerman (1979)
D_{CH4}	2×10^{-5} cm^2 s^{-1}	Lerman (1979)
D_{O2}	1.96×10^{-5} cm^2 s^{-1}	Lerman (1979)
r_{org}	0.01097	δ^{13}C of C3 plants = −27‰
$\alpha_{prod \rightarrow dic}$	Aceticlastic = 0.98 CO_2-red = 0.945	Whiticar (1999)
$\alpha_{prod \rightarrow ch4}$	Aceticlastic = 1.02 CO_2-red = 1.055	We assume a ratio of 75/25 acetate/CO_2-reduction, consistent with Whiticar (1986)
$\alpha_{ox \rightarrow dic}$	1.01	*Ibid*
$\alpha_{ox \rightarrow dic}$	0.99	*Ibid*
Porosity	0.9	No direct assessment of porosity was made
H_{CO2}	3.4×10^{-2}mol L^{-1} atm^{-1}	Morel & Hering (1993)
H_{CH4}	1.3×10^{-3}mol L^{-1} atm^{-1}	Morel & Hering (1993)

when the model reproduced the $\delta^{13}C_{CO2}$ profiles but underestimated the $CO_{2(aq)}$ concentration profiles. Similar to the respiration terms, two alternate transport functions were built into the model, which were only active when the modelled CH_4 concentrations exceeded the concentrations observed in the data. The first removed a given proportion of the CH_4 in each box from 0 to 40 cm below the peat surface at each time step. The second transport function also removed gases proportional to their concentrations from 0 to 50 cm, removing 75% of the CH_4 and 45% of the CO_2, but, when employed, this function is only active for a single time step.

Boundary conditions

Surface boundary conditions: the concentrations in box $z = 1$ were assumed to be at equilibrium with the atmosphere at the beginning of each time step, in accordance with the Henry's law constants for each gas species, modified by the surface temperature. The bottom boundary was treated as a no-flux boundary at 100 cm.

RESULTS

Throughout the year, the concentration profiles show low CO_2 and CH_4 concentrations near the surface that quickly increase and then begin to level off between 10 and 40 cm, depending on the season. The CH_4 concentrations show considerable variability between the two vials collected at the same depth. Quantifying the samples, we have noted that the first vial collected usually has higher CH_4 concentrations (but only very slightly higher CO_2 concentrations) than the second vial collected. We interpret this as the preferential sampling of bubbles in the first vial, which represents the *dissolved + gaseous* concentration, while the second vial is closer to the *dissolved* concentration. In contrast, the CO_2 concentrations have much less scatter in the top 40 cm. Below this, the CO_2 profiles occasionally show increased variability, depending on the season. Throughout the year, methane concentrations approach and exceed saturation whereas CO_2 remains below saturation in the pore waters sampled. For this reason, we suggest that it is not appropriate to think of this concentration difference between replicate vials as a measurement error, but rather as further indication that methane moves through the pore waters in non-diffusive ways.

The carbon isotope profiles we measured from fen pore waters were characterized by depletion in ^{13}C content near the surface and enrichment in ^{13}C at depth (Fig. 1), which is consistent with a diffusion-dominated system. The depleted portion of the curve was most prominent during the winter, extending through the top 40 cm of saturated peat. The depth of the ^{13}C-depleted region grew shallower throughout the year almost disappearing in August and then growing again through the fall. The near surface depletion in ^{13}C reached its most negative values during the early fall, peaking at −25‰ on 2 October, while remaining near −20‰ throughout the winter and spring. During the summer months, however, the isotopic depletion became less pronounced with values of −15‰ at 2.5 cm. In the spring and late fall, the $\delta^{13}C$ profiles are characterized by a second zone of depletion in ^{13}C occurring below the first enrichment zone.

We find distinct seasonal variability in the rates of methane production and oxidation over the course of the year (Fig. 1), with the model explaining over 80% of the variability in the carbon isotope data (see Appendix S1). Maximum methane production rates varied between 0 and 67 nmol cm^{-3} day^{-1}, depending on the season. Throughout most of the year, we found multiple peaks in methane production. We found no evidence for any significant methane production occurring between these peaks where none is displayed, although some low-level methane production may not be resolvable if it is more than 1 order of magnitude below the peak rates. During the winter months, we found only a deep zone of methanogenesis occurring approximately 50 cm below the depth of saturation. In the spring, methane production shoaled towards the top of the pore water profile until August during which methane production was active primarily in the top 10 cm. During the fall, methane production reversed this trend and pushed deeper into the profile leading back to the winter methanogenic pattern. The high rates of methane

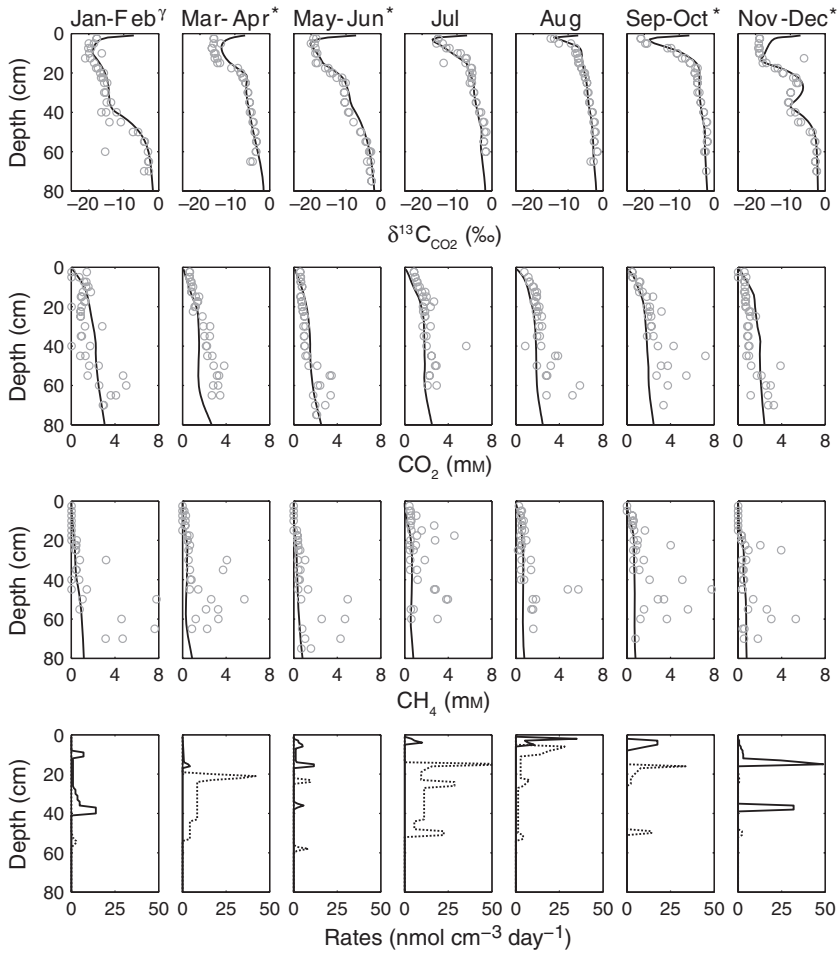

Fig. 1 Data from Sallies Fen presented with model results. The top row shows the isotopic composition of the pore water CO_2 with depth in grey circles, as well as the model results in black lines, for selected months. The second and third rows show the CO_2 and CH_4 concentrations, respectively, compared with the model results. Concentrations are displayed in units of mmol L^{-1} and isotopic compositions in delta notation. The fourth row shows the profiles of CH_4 production and oxidation rates used to obtain the model results shown in the top three rows. Empty outlines indicate methanotrophy rates and dashed outlines indicate methanogenesis rates in units of nmol cm^{-3} day^{-1}. $^{\gamma}$Without data profiles for January and March 2006, this column represents the sampled data from February and the model values for January, February and March. *These columns represent months that were compressed due to similarity. The results shown are the data and model results for the first of the 2 months listed. We chose not to display the second month for compactness and because few rate changes were necessary to match essentially identical data profiles.

production over a broad depth region during the month of June are a direct result of the existence of the second zone of isotopic depletion that occurred during the spring. Other than this feature, and the transition between winter and spring, the depth-integrated rates of methane production remained remarkably constant throughout the year.

The magnitude of the peak methane oxidation rates were also found to vary over the season with maximum rates, reaching 50 nmol cm^{-3} day^{-1} in November (Fig. 1). The zone of methane oxidation shifted vertically in the pore water profile, similar to methane production, also showing a seasonal second zone of activity at 40 cm during the spring and fall. During the summer months, it was more difficult to separate methanotrophy from oxic respiration due to the narrow, shallow oxic zone. Separating these processes relies on the concentration profiles, which may have only one data point (at 2.5 cm) in this region. It is also important to note that higher rates of methane oxidation may have been present either in the top several centimetres of the pore water or, more likely, in the unsaturated peat layer that would not be resolved using this sampling technique. Production rates of CO_2 via respiration were also estimated, varying between 0 and 8 nmol cm^{-3} day^{-1} with peak rates found in the winter months followed by an absence of respiration rates during the spring (Fig. 2). We estimated respiration and methane oxidation rates to be roughly equal from July through October.

Sensitivity tests were run to examine how the alternate transport term impacted the concentration profiles and emission across the modelled surface (see Appendix S1). For example, complete removal of the alternate transport term increased the diffusive flux in the subsequent months, although total predicted emissions declined and the concentration profiles during those months overestimated the observed concentrations. We found that the profiles were reproduced best using a gas-release event in March. Replacing this 'event' with the constant removal of methane, each timestep still resulted in better fits to the data than using only diffusive transport. We find that total emissions, in addition to the seasonal pattern of methane emissions from the model, are highly dependent on these non-diffusive transport terms. Additionally, high methane emissions are not directly correlated to times of high methane production (unless the production occurs very close to the surface) due to the long diffusive time scale. For these reasons, we find it more useful to focus

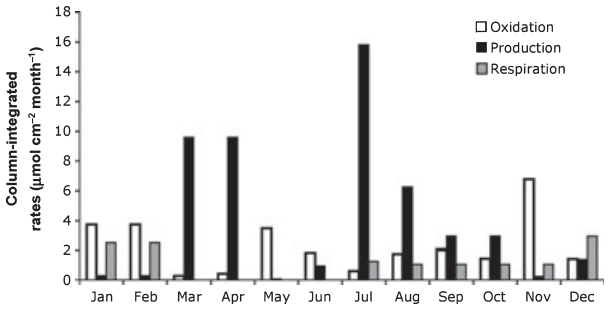

Fig. 2 Column-integrated rates of methane production, oxidation and respiration for each month. Values are monthly integrated and shown in units of μmol cm^{-2} $month^{-1}$.

Table 2 Comparing the model to observations

	μmol cm^{-2} $year^{-1}$*
Static flux chamber emissions	491
Model production rates	50
Model oxidation rates	27
Model flux	70

*These represent rates and emissions April through December only in order to compare with observed fluxes.

on the column-integrated rates of methane production and oxidation, rather than modelled methane flux.

We compared our column-integrated net methane production rates with static flux chamber emissions data taken at this site (R. K. Varner and P. M. Crill, unpublished data). Although we would not expect them to match perfectly, on an annual time scale, the amount of methane produced should approximately equal the amount of methane released. The comparison can be seen in Table 2. As can be seen, the isotope-derived production rates cannot account for the observed fluxes (the majority of which come between July and September). The isotope-constrained annual net methane production is approximately 20 times too low to account for this level of annual emissions. No winter (January–March) static flux chamber data were available from 2006 but winter emissions are likely to be small (see December flux rates). Although the CH_4 flux measured at this site in 2006 is higher than the average yearly flux at this site, neither the flux numbers, nor the cumulative production, are anomalous. Preliminary results from other years and other stations show a similar trend with insufficient methane production rates to account for observed fluxes.

DISCUSSION

Throughout much of the year, we found multiple discrete peaks of methane production in the peat. It is possible that the peaks represent contributions from the two different types of methanogenesis, with acetoclastic methanogenesis driving the near-surface peaks, and CO_2-reduction dominating at depth. This hypothesis is supported by methane and CO_2 isotope data by Hornibrook *et al.* (2000) showing an analogous switch in production pathways with depth from several different sites. However, if it is the case that the two peaks represent different pathways, it is not clear why they are separated by depth or why acetoclastic methanogenesis would be limited to such a shallow depth range. If H_2 is being produced deeper, enabling CO_2-reduction, those same fermentative processes lead to acetate production as an end member. Other possibilities for the separate methanogenic peaks include seasonal dynamics in the production of substrates or nutrients that results in pulses available to varying depths, or ecological competition between microbial communities affecting methanogenic productivity.

The isolated second region of isotopic depletion that occurs during several months of the spring and fall is slightly more difficult to interpret. We did not feel that we could ignore the region, as it significantly impacts the rates of methane production needed to reproduce the following month's profile, as mentioned earlier. The only way to reproduce these curves successfully using the model was to add a second zone of methane oxidation into the profile. It has previously been suggested that plant roots leak oxygen into the surrounding peat through their aerenchyma (Thomas *et al.*, 1996). Such a mechanism could be responsible for bringing sufficient oxygen to these depths to drive a local peak in methanotrophy. Alternatively, a rapidly rising water table (as occurred in November) could create a thick oxygenated layer. Due to high near-surface rates of decomposition, the top centimetres may re-establish anoxia before the intermediate region, resulting in a profile such as the one observed during the late fall. Similar regions of negative production were also found in a recent study by Beer *et al.* (2008), although they suggest these regions may caused by their steady-state assumption. It is also possible that, in our study, this pattern is an artefact of the monthly sampling time scale. Microbial processes occur on a much shorter time scale and our method represents a time-integration of these microbial activities over that month. Therefore, we do not need to imply that methane oxidation occurred concurrently below a zone of methane production, only that net methane oxidation and net methane production occurred at the depths indicated.

This method of using the $\delta^{13}C$ profiles of aqueous CO_2 to calculate the rates of methane production and oxidation not only has several advantages over previous methodologies but also comes with certain limitations. An important advantage is that the acquired rates of methane production and oxidation are independent of the CH_4 concentration profiles. This is advantageous due to the low solubility of methane causing large variability in these profiles and because the CH_4 concentration profiles can be used to explore the importance of non-diffusive transport. However, there are also limitations to this approach. For example, both methane oxidation and oxic respiration (degradation or plant respiration) add depleted

carbon to the pore water profile and therefore must be distinguished using the CO_2 concentration profiles, which are also needed to calculate all the rates. Additionally, this method only allows calculation of the microbial rates occurring in the saturated peat, ignoring potentially significant activity in the unsaturated peat. This is not only particularly problematic for methane oxidation but may also cause the underestimation of methanogenesis rates, a potential source of uncertainty that will be discussed below.

The largest mystery in our study is how to reconcile the isotope profiles of the dissolved $CO_{2(aq)}$ with the emission data. Non-diffusive transport cannot be the solution. Neither the concentration nor the isotope data are consistent with advection being an important influence in this system. Advection would wipe out all the observed gradients and, during every season, this is not the case (Fig. 1). This is also in agreement with results from Beer & Blodau (2007) that found diffusion to dominate transport in their peatland study site. Another possible source of error is the assumption of constant porosity with depth; however, unless the porosity was to increase with depth, this would only result in overestimation of the rates of methanogenesis with depth rather than underestimation.

If the isotopic fractionation associated with methanogenesis during the summer is much smaller than previous estimates, resulting in minimal effect on the pore water $\delta^{13}C$ of the $CO_{2(aq)}$, then it might be possible to produce CH_4 that would not be observed by our system. However, such methanogenesis would still produce $CO_{2(aq)}$, meaning that we should observe resulting peaks in our concentration profiles. The same argument holds for methane produced using any methylated substrate (including methylamines and dimethyl sulfide). The aqueous CO_2 concentration profiles are also inconsistent with the argument that subsurface respiration (root respiration, for example) could necessitate much higher rates of methane production at those same depths to reproduce the isotope profiles. In each case, although the CH_4 may escape observation, if it is rapidly transported out either by bubbling or plant transport, the $CO_{2(aq)}$ should be largely unaffected. Measurements of gas concentrations in wetland bubbles support this principle, having been found to contain only 4–12% CO_2 compared with 24–70% CH_4 (Rothfuss & Conrad, 1994; Shannon *et al.*, 1996; Tokida *et al.*, 2007). Therefore, high subsurface rates of methanogenesis are not consistent with the $CO_{2(aq)}$ profiles we observe, which are within the range found in other wetlands (Crill *et al.*, 1988; Christensen *et al.*, 1996; MacDonald *et al.*, 1998; Frolking *et al.*, 2001; Walter *et al.*, 2001).

Decreasing the fractionation factor associated with methane production towards zero would also require the CH_4 emitted from Sallie's Fen to be isotopically heavier than any CH_4 previously observed from wetland systems, almost identical to the source biomass. Preliminary measurements of $\delta^{13}C_{CH4}$ from a selection of our samples supported the fractionation factor used by in our modelling study with values between −54‰ and −62‰. Furthermore, there is an intramolecular gradient within acetate that is likely to result in produced CO_2 being at least 5–10‰ enriched relative to the bulk organic matter (Rossmann *et al.*, 1991; Sugimoto & Wada, 1993; Gelwicks *et al.*, 1994; Penning *et al.*, 2006).

Errors in the assumed isotopic fractionations associated with either fermentation or methane oxidation also cannot help to explain the observed discrepancy. As described earlier, we used the common assumption that heterotrophic respiration does not significantly fractionate organic matter (~1–2‰; Balesdent *et al.*, 1987; Penning & Conrad, 2006). Recently, some studies of soil respiration have found differences between soil organic carbon and respired CO_2, indicating an isotopic fractionation of ±6‰ (Santruckova *et al.*, 2000; Conrad *et al.*, 2009). This, however, remains unconstrained and may be a transient observation as different soil fractions either build up or are metabolized. For the purposes of this study, such a small fractionation does not add significantly to our uncertainties. The fractionation associated with methane oxidation has also been found to vary, greatly exceeding our assumed value of 10‰ at high local methane concentrations (Teh *et al.*, 2006). First, it is unlikely that this variability would exceed our already large uncertainties and, second, it would have no impact on our principle finding: we could reduce all methane oxidation rates to zero and the model still cannot produce sufficient methane and remain consistent with the pore water carbon isotope data.

One possible explanation for the high summer emissions, beyond what can be justified by isotopic constraints, is that there are very high rates of CH_4 production occurring in the unsaturated peat and/or the top several centimetres of the saturated peat (possibly associated with the oxic/anoxic boundary) that is rapidly equilibrated with the atmosphere through gas exchange. The rapid gas exchange in this region would remove the residual CO_2, enriched in ^{13}C, such that no record of this methane production would be preserved in the pore-fluid profiles that we measure. We hypothesize that the close proximity of an oxic boundary may be necessary to support high rates of acetate (and possibly also H_2) production, either because of the favourable redox gradient or because oxygen speeds up the degradation of complex organic molecules such that, upon experiencing anoxic conditions, methanogenic substrates can be produced at enhanced rates. Furthermore, if this were correct, it would mean that the majority of methane released by Sallie's Fen is produced in, or above, the top 1–3 cm of the pore water profile.

The idea that wetland methanogenesis rates peak at shallow depths is not heretical, a variety of incubation studies during the last 20 years found that methane production rates were highest in the near-surface samples (King *et al.*, 1981; Sansone & Martens, 1981; Svensson & Rosswall, 1984; Williams & Crawford, 1984; Brown *et al.*, 1989; Moore &

Knowles, 1990; Valentine *et al.*, 1994; Bergman *et al.*, 2000; Dettling *et al.*, 2007). Brown (1998) further noted that incubated catotelm peat appeared to inhibit methanogenesis if combined with high methane-producing acrotelm peat. Clymo & Pearce (1995) suggested that methane production may be greatest in the 'transition zone' between oxia and anoxia (between 4 and 15 cm below the water table). Several *in situ* techniques based on modelling concentration profiles have also supported this hypothesis (Beer *et al.*, 2008; Clymo & Bryant, 2008). As mentioned earlier, it is also possible that high rates of methanogenesis could occur above the water table in micro-anaerobic zones within the unsaturated peat, consistent with work by Tokida *et al.* (2007) that found net methane production in soils with moisture contents as low as 60%. Additionally, there are parallels with studies of microbial mat systems showing high rates of anaerobic activity (sulphate reduction and methanogenesis) in the oxic top millimetres of the microbial mat (Canfield & Desmarais, 1991; Buckley *et al.*, 2008).

In order to assess whether methane production rates of this magnitude are possible, we compared the rate estimates derived from this study, and those that would be required in the near-surface peat, to previous estimates of potential methane production derived from laboratory incubations. The mean methane production rate calculated in this study, 0.18 μmol cm^{-3} $month^{-1}$ (averaged for all depths above 25 cm from July to September) is lower than the average potential methane production (PMP) value derived by incubation experiments (0.32 μmol cm^{-3} $month^{-1}$ for oligotrophic systems) (see review by Segers, 1998). Although there are many reasons to believe *in situ* rates may differ substantially from laboratory-derived PMP rates, the average (non-zero) rate of methane production calculated in this study, 0.32 μmol cm^{-3} mo^{-1}, is similar to the mean compiled above. Therefore, explaining the discrepancy between the carbon isotope data and the observed methane emissions would require near-surface production rates that are 3 orders of magnitude higher than these compiled subsurface rates. However, most incubation studies pool between 5 and 15 cm of vertical depth for each incubation and rarely include the surface centimetres of peat for methane production potentials. One study on Everglades peat and marl soils (omitted from the above review as an outlier due to the high values and hot incubation temperatures) incubated the top 0 to 2 cm and found methane production rates of 1800–7200 μmol cm^{-3} $month^{-1}$, approximately an order of magnitude higher than the methane production rates we estimate would be necessary to account for the missing methane production.

Further research either with incubations designed to isolate the impact of the oxic/anoxic interface, assessment of the microbial community composition of these near-surface samples, or high depth-resolution continuous sampling of gas concentrations and isotopic compositions *in situ* is necessary to find additional support for this mechanism.

CONCLUSIONS

Using measurements of the $\delta^{13}C$ of $CO_{2(aq)}$ in pore fluids, we calculate methane production and oxidation rates in a New Hampshire wetland over the course of a seasonal cycle. Methanogenesis occurs in distinct peaks with depth between which there is little or no methane production. During the winter, CH_4 production occurs deeper (>40 cm) and shoals to shallow depths in the summertime (5–20 cm). The methane production rates, constrained by the $\delta^{13}C_{CO2}$ measurements, cannot account for the high emission rates in the summer. We propose that most summertime methane production occurs either in the upper 1–3 cm of saturated peat, or the unsaturated peat, leaving no isotopic signal because of frequent equilibration with the atmosphere driven by episodic mixing.

ACKNOWLEDGEMENTS

We would like to thank Dr Ruth Varner and Dr Patrick Crill for access to Sallie's Fen, which is supported by the National Science Foundation as an LTREB site (DEB-0316326). This work was supported by the Merck Fund of the New York Community Trust.

REFERENCES

Balesdent J, Mariotti A, Guillet B (1987) Natural C-13 abundance as a tracer for studies of soil organic-matter dynamics. *Soil Biology and Biochemistry* **19**, 25–30.

Beer J, Blodau C (2007) Transport and thermodynamics constrain belowground carbon turnover in a northern peatland. *Geochimica et Cosmochimica Acta* **71**, 2989–3002.

Beer J, Lee K, Whiticar M, Blodau C (2008) Geochemical controls on anaerobic organic matter decomposition in a northern peatland. *Limnology and Oceanography* **53**, 1393–1407.

Berg P, Risgaard-Petersen N, Rysgaard S (1998) Interpretation of measured concentration profiles in sediment pore water. *Limnology and Oceanography* **43**, 1500–1510.

Bergman I, Svensson BH, Nilsson M (1998) Regulation of methane production in a Swedish acid mire by pH, temperature and substrate. *Soil Biology and Biochemistry* **30**, 729–741.

Bergman I, Dlarqvist M, Nilsson M (2000) Seasonal variation in rates of methane production from peat of various botanical origins: effects of temperature and substrate quality. *FEMS (Federation of European Microbiological Societies) Microbiology – Ecology* **33**, 181–189.

Berner RA (1980) *Early Diagenesis: A Theoretical Approach.* Princeton University Press, Princeton, NJ.

Blodau C, Moore TR (2003) Micro-scale CO2 and CH4 dynamics in a peat soil during a water fluctuation and sulfate pulse. *Soil Biology and Biochemistry* **35**, 535–547.

Brown DA (1998) Gas production from an ombrotrophic bog – effect of climate change on microbial ecology. *Climatic Change* **40**, 277–284.

Brown A, Mathur SP, Kushner DJ (1989) An ombrotrophic bog as a methane reservoir. *Global Biogeochemical Cycles* **3**, 205–213.

Bubier JL (1995) The relationship of vegetation to methane emission and hydrochemical gradients in northern peatlands. *Journal of Ecology* **83**, 403–420.

Buckley DH, Baumgartner LK, Visscher PT (2008) Vertical distribution of methane metabolism in microbial mats of the Great Sippewissett Salt Marsh. *Environmental Microbiology* **10**, 967–977.
Canfield DE, Desmarais DJ (1991) Aerobic sulfate reduction in microbial mats. *Science* **251**, 1471–1473.
Christensen TR, Prentice IC, Kaplan J, Haxeltine A, Sitch S (1996) Methane flux from northern wetlands and tundra – an ecosystem source modelling approach. *Tellus Series B: Chemical and Physical Meteorology* **48**, 652–661.
Clymo RS, Bryant CL (2008) Diffusion and mass flow of dissolved carbon dioxide, methane, and dissolved organic carbon in a 7-m deep raised peat bog. *Geochimica et Cosmochimica Acta* **72**, 2048–2066.
Clymo RS, Pearce DME (1995) Methane and carbon-dioxide production in, transport through, and efflux from a peatland. *Philosophical Transactions of the Royal Society of London. Series A: Mathematical and Physical Sciences* **351**, 249–259.
Conrad R (1989) Control of methane production in terrestrial ecosystems. In *Exchange of Trace Gases Between Terrestrial Ecosystems and the Atmosphere* (eds Andreae MO, Schimel DS). Wiley & Sons, Ltd, New York, NY, pp. 39–58.
Conrad R (2002) Control of microbial methane production in wetland rice fields. *Nutrient Cycling in Agroecosystems* **64**, 59–69.
Conrad R, Claus P, Casper P (2009) Characterization of stable isotope fractionation during methane production in the sediment of a eutrophic lake, Lake Dagow, Germany. *Limnology and Oceanography* **54**, 457–471.
Crill PM, Bartlett KB, Harriss RC, Gorham E, Verry ES, Sebacher DI, Madzar L, Sanner W (1988) Methane flux from Minnesota peatlands. *Global Biogeochemical Cycles* **2**, 371–394.
Denman KL, Brasseur G, Chithaison A, Clais P, Cox PM, Dickenson RE, Hauglustaine D, Heinze C, Holland E, Jacob D, Lohmann U, Ramachandran S, Dias DS, Wofsy SC, Zhang X (2007) Climate change 2007: the physical science basis. In *Contribution of Working Group 1 to the Fourth Assessment Report of the Intergovernmental Panel on Climate Change* (eds Solomon S, Qin D, Manning M, Chen Z, Marquis M, Averyt KB, Tignor M, Miller HL). Cambridge University Press, Cambridge, UK and New York, NY, USA.
Dettling MD, Yavitt JB, Cadillo-Quiroz H, Sun C, Zinder SH (2007) Soil-methanogen interactions in two peatlands (bog, fen) in central New York State. *Geomicrobiology Journal* **24**, 247–259.
Duval B, Goodwin S (2000) Methane production and release from two New England peatlands. *International Microbiology* **3**, 89–95.
Ferry JG (1992) Methane from acetate. *Journal of Bacteriology* **174**, 5489–5495.
Frolking S, Crill P (1994) Climate controls on temporal variability of methane flux from a poor fen in southeastern New Hampshire: measurement and modeling. *Global Biogeochemical Cycles* **8**, 385–397.
Frolking S, Roulet NT, Moore TR, Richard PJH, Lavoie M, Muller SD (2001) Modeling northern peatland decomposition and peat accumulation. *Ecosystems* **4**, 479–498.
Gelwicks JT, Risatti JB, Hayes JM (1994) Carbon isotope effects associated with aceticlastic methanogenesis. *Applied and Environmental Microbiology* **60**, 467–472.
Goodwin S, Zeikus JG (1987) Physiological adaptations of anaerobic-bacteria to low pH – metabolic control of proton motive force in Sarcina-ventriculi. *Journal of Bacteriology* **169**, 2150–2157.
Hein R, Crutzen PJ, Heimann M (1997) An inverse modelling approach to investigate the global atmospheric methane cycle. *Global Biogeochemical Cycles* **11**, 43–76.
Holzapfel-Pschorn A, Conrad R, Seiler W (1986) Effects of vegetation on the emission of methane from submerged paddy soil. *Plant and Soil* **92**, 223–233.
Hornibrook ERC, Longtaffe FJ, Fyfe WS (2000) Evolution of stable carbon isotope compositions for methane and carbon dioxide in freshwater wetlands and other anaerobic environments. *Geochimica et Cosmochimica Acta* **64**, 1013–1027.
Kang H, Freeman C (2002) The influence of hydrochemistry on methane emissions from two contrasting northern wetlands. *Water, Air, & Soil Pollution* **141**, 263–272.
King GM, Berman T, Wiebe WJ (1981) Methane Formation in the Acidic Peats of Okefenokee Swamp, Georgia. *American Midland Naturalist* **105**, 386–389.
Lerman A (1979) *Geochemical Properties: Water and Sediment Environments.* John Wiley & Sons, Inc., New York, NY.
MacDonald JA, Fowler D, Hargreaves KJ, Skiba U, Leith ID, Murray MB (1998) Methane emission rates from a northern wetland; response to temperature, water table and transport. *Atmospheric Environment* **32**, 3219–3227.
Melloh RA, Crill PM (1996) Winter methane dynamics in a temperate peatland. *Global Biogeochemical Cycles* **10**, 247–254.
Moore TR, Knowles R (1990) Methane emissions from fen, bog and swamp peatlands in Quebec. *Biogeochemistry* **11**, 45–61.
Morel FMM, Hering JG (1993) *Principles and Applications of Aquatic Chemistry.* Wiley, Wiley-Interscience.
Penning H, Conrad R (2006) Carbon isotope effects associated with mixed-acid fermentation of saccharides by Clostridium papyrosolvens. *Geochimica et Cosmochimica Acta* **70**, 2283–2297.
Penning H, Claus P, Casper P, Conrad R (2006) Carbon isotope fractionation during acetoclastic methanogenesis by Methanosaeta concilii in culture and a lake sediment. *Applied and Environmental Microbiology* **72**, 5648–5652.
Phelps TJ, Zeikus JG (1984) Influence of pH on terminal carbon metabolism in anoxic sediments from a mildly acidic lake. *Applied and Environmental Microbiology* **48**, 1088–1095.
Rossmann A, Butzenlechner M, Schmidt HL (1991) Evidence for a nonstatistical carbon isotope distribution in natural glucose. *Plant Physiology* **96**, 609–614.
Rothfuss F, Conrad R (1994) Development of a gas-diffusion probe for the determination of methane concentrations and diffusion characteristics in flooded paddy soil. *FEMS (Federation of European Microbiological Societies) Microbiology – Ecology* **14**, 307–318.
Sansone FJ, Martens CS (1981) Methane production from acetate and associated methane fluxes from anoxic coastal sediments. *Science* **211**, 707–709.
Santruckova H, Bird MI, Lloyd J (2000) Microbial processes and carbon-isotope fractionation in tropical and temperate grassland soils. *Functional Ecology* **14**, 108–114.
Schrag DP, DePaulo DJ (1993) Determination of δ18O of seawater in the deep ocean during the last glacial maximum. *Paleoceanography* **8**, 1–6.
Segers R (1998) Methane production and methane consumption: a review of processes underlying wetland methane fluxes. *Biogeochemistry* **41**, 23–51.
Shannon RD, White JR, Lawson JE, Gilmour BS (1996) Methane efflux from emergent vegetation in peatlands. *Journal of Ecology* **84**, 239–246.
Sivan O, Schrag DP, Murray RW (2007) Rates of methanogenesis and methanotrophy in deep-sea sediments. *Geobiology* **5**, 141–151.
Smith KA, Ball T, Conen F, Dobbie KE, Massheder J, Rey A (2003) Exchange of greenhouse gases between soil and atmosphere: interactions of soil physical factors and biological processes. *European Journal of Soil Science* **54**, 779–791.
Sugimoto A, Wada E (1993) Carbon isotopic composition of bacterial methane in a soil incubation experiment – contributions of

acetate and CO_2/H_2. *Geochimica et Cosmochimica Acta* **57**, 4015–4027.
Svensson BH, Rosswall T (1984) Insitu methane production from acid peat in plant-communities with different moisture regimes in a subarctic mire. *Oikos* **43**, 341–350.
Teh YA, Silver WL, Conrad ME, Borglin SE, Carlson CM (2006) Carbon isotope fractionation by methane-oxidizing bacteria in tropical rain forest soils. *Journal of Geophysical Research* **111**, G01003.
Thomas KL, Benstead J, Davies KL, Lloyd D (1996) Role of wetland plants in the diurnal control of CH4 and CO2 fluxes in peat. *Soil Biology and Biochemistry* **28**, 17–23.
Tokida T, Miyazaki T, Mizoguchi M, Nagata O, Takakai F, Kagemoto A, Hatano R (2007) Falling atmospheric pressure as a trigger for methane ebullition from peatland. *Global Biogeochemical Cycles* **21**, GB2003.
Treat CC, Bubier JL, Varner RK, Crill PM (2007) Timescale dependence of environmental and plant-mediated controls on CH4 flux in a temperate fen. *Journal of Geophysical Research. G, Biogeosciences* **112**, G01014.
Valentine DW, Holland EA, Schimel DS (1994) Ecosystem and Physiological Controls over Methane Production in Northern Wetlands. *Journal of Geophysical Research-Atmospheres* **99**, 1563–1571.
Walter BP, Heimann M (2000) A process-based, climate-sensitive model to derive methane emissions from natural wetlands: application to five wetland sites, sensitivity to model parameters, and climate. *Global Biogeochemical Cycles* **14**, 745–765.
Walter BP, Heimann M, Shannon RD, White JR (1996) A process-based model to derive methane emissions from natural wetlands. *Geophysical Research Letters* **23**, 3731–3734.
Walter BP, Heimann M, Matthews E (2001) Modelling modern methane emissions from natural wetlands 2. Interannual variations 1982–1993. *Journal of Geophysical Research* **106**, 34, 207–234, 219.
Whiticar MJ, Faber E, Schoell M (1986) Biogenic methane formation in marine and freshwater environments: CO_2 reduction vs. acetate fermentation – Isotope evidence. *Geochim. Cosmochim. Acta* **50**, 693–709.
Whiticar MJ (1999) Carbon and hydrogen isotope systematics of bacterial formation and oxidation of methane. *Chemical Geology* **161**, 291–314.
Whiting GJ, Chanton JP (1992) Plant-dependent CH4 emission in a subarctic Canadian fen. *Global Biogeochemical Cycles* **6**, 225–231.
Williams RT, Crawford RL (1984) Methane production in Minnesota Peatlands. *Applied and Environmental Microbiology* **47**, 1266–1271.
Wuebbles DJ, Hayhoe K (2002) Atmospheric methane and global change. *Earth Science Reviews* **57**, 177–210.

SUPPORTING INFORMATION

Additional Supporting Information may be found in the online version of this article:

Appendix S1. Results from sensitivity analyses.

Please note: Wiley-Blackwell is not responsible for the content or functionality of any supporting materials supplied by the authors. Any queries (other than missing material) should be directed to the corresponding author for the article.